J. COMBIN. MATH. COMBIN. COMPUT. 127b (2025) 8565--8579

Journal of Combinatorial Mathematics and Combinatorial Computing
www.combinatorialpress.com/jcmcc

Research on trajectory planning and control of flying robotic arm based on image moments and deep learning vector product

Yang Li[1,✉], Wenzhuo Yang[1], Yongqi Wang[1], Chengjun Chen[1], Guangzheng Wang[1], Xuefeng Zhang[1]

[1] *School of Mechanical and Automotive Engineering, Qingdao University of Technology, Qingdao, Shandong, 266520, China*

ABSTRACT

With the development of science and technology, the application of flight manipulators has received extensive attention. The flying manipulator has broad application prospects, such as the maintenance of high-voltage towers, the storage and retrieval of elevated goods in warehouses, and the delivery of express and takeout goods. Before the actual application of the flight manipulator, due to the complex task requirements and nonlinear environment, it is necessary to continuously optimize the Trajectory Planning and Control (hereinafter referred to as TPC) of the flight manipulator. In order to improve the recognition and positioning accuracy of the robotic arm on the surface of the aircraft, and achieve precise control of the autonomous motion and operation of the robotic arm on the surface of the aircraft, this paper studies the TPC of the flight robotic arm based on deep learning, image moment and vector product methods, establishes a bearing return function model based on deep learning, and a Jacobian matrix of the flight robotic arm based on image moment and vector product methods. Through the experimental research on TPC of the flight manipulator, it was proved that the DL trajectory planning method could reduce the collision risk of the flight manipulator by 4.79% compared with the traditional trajectory planning method, and could improve the task completion speed of the flight manipulator by 4.66%. The application of DL to the TPC of the flight manipulator could improve the trajectory planning effect of the flight manipulator.

Keywords: Deep Learning, Image Moment, Vector Product Method, Flight Robotic Arm Trajectory Planning, Blockchain Technology

✉ Corresponding author.
E-mail address: yuemingxingxi_1231@163.com (Y. Li).
Received 01 March 2024; Revised 25 May 2024; Accepted 10 November 2024; Published Online 16 April 2025.
DOI: 10.61091/jcmcc127b-469

1. Introduction

Thanks to the high-speed development of microelectronic technology, UAVs have gradually become the object of researchers' favor by virtue of the characteristics of low manufacturing cost, strong adaptability and high flexibility. It will be gradually intelligentized, simplified, multifunctional and even clustered, and is widely used in transportation, agriculture and aerial photography and other fields [1-3]. However, these jobs have a limited ability to interact with the environment, and UAVs are more about sensing and observing the world, limiting the use of UAVs. However, operational robots on the ground shine in the fields of underwater, construction site work, earthquake relief, and anti-terrorism and explosion prevention [4-7]. In order to meet the people's material and cultural needs, researchers have begun to carry active robotic arms on UAVs, and flying robotic arm systems have emerged. Compared with traditional drones, flying robotic arms can actively interact with the environment, which greatly broadens the use of drones [8-11]. Such as entering high-risk environments instead of manual tasks, completing sample sampling in uninhabited areas, multiple flying robotic arms can even complete cooperative handling, assembly and even constitute large aircraft with the help of controllers, and so on. Changes in the structure of UAVs have brought new challenges to researchers [12-14]. On the one hand, it is hoped that the flying robotic arm will have a longer endurance and be able to accomplish more operational tasks. On the other hand, it is necessary to carry more complex robotic arms on the UAV, with better endurance and heavier power supply system, which leads to the coupling effect brought by the robotic arms that researchers have to take into account when doing the system modeling, trajectory planning, and motion control of the flying robotic arms [15-17]. Considering that the lightweighting of UAV mechanism and power supply system has gradually matured in the market, the flying robotic arm can only be made longer-lasting and more capable of operation by lightweighting the robotic arm and simplifying its structure. The traditional robotic arm structure is bulky and high energy consumption, which will greatly affect the endurance of the flying robotic arm [18-20]. When performing operational tasks, the larger rotational inertia will disturb the UAV, which will then reduce the positioning accuracy and operational capability of the flying robotic arm, and even lead to the damage of the flying robotic arm in serious cases [21-22]. In this regard, image moment and deep learning vector product techniques can be innovatively introduced into the system modeling, trajectory planning, and motion control design of the flying robotic arm to develop a new flying robotic arm, which can effectively improve the problems of poor range, large disturbance, and difficult to control inherent in the traditional flying robotic arm, and then realize its high-quality operation in the air [23-25].

In order to improve the trajectory planning effect of flying robots, enhance the mechanization and learning ability of control modes, this paper uses DL, image moment, and vector product methods to study the TPC of flying robots. In this paper, an azimuth reward function model based on DL was proposed, and the Jacobian matrix of the flight manipulator based on image moment and vector product method was constructed. This paper discussed the application of blockchain technology in the data security of flying robots, and conducted empirical research from the following aspects: collision evaluation of flying robots, speed evaluation of flying robots reaching the target point, evaluation of comprehensive collision times and time of reaching the target point, and data security evaluation. To verify the effectiveness of image moments and deep learning vector product methods, this article evaluates flying robots from collision testing, speed testing, safety testing, and other aspects. In terms of collision testing, the average collision test evaluation index of flying robots under DL trajectory planning method is 3.58 higher than that under traditional trajectory planning method, with a proportion of 4.79% higher; At the speed testing level, the average speed evaluation index of the flight robot under the traditional trajectory planning method is 73.22, while the average speed evaluation index of the flight robot under the DL trajectory planning method is 76.63. Compared with traditional trajectory planning, the speed evaluation index of general flight robots under the DL trajectory planning method is 3.41 higher, with a proportion of 4.66% higher. At the security testing level, the data security evaluation index for flight robots using conventional technology is 74.04, and the data security evaluation index for flight robots using blockchain technology is 79.17. Compared with conventional technologies, the data security evaluation index of flying robots using blockchain technology is 5.13% higher, with a proportion of 6.93% higher. From the results, it can be seen that the trajectory planning and control of flight robotic arms based on image moments and deep learning vector products have higher sensitivity and safety, and can demonstrate higher value in practical applications.

2. Flight Robot Trajectory Planning Based on Deep Learning

In this paper, the DL reward function is studied to improve the robustness of flight manipulator trajectory planning. The reward function includes position function and direction function.

1) Position reward function. For the flight robot arm, it is necessary to execute the command quickly and avoid obstacles to protect itself from damage. Therefore, the location function includes two aspects: One is to avoid obstacles, and the other is to guide the target. The obstacle avoidance item helps the flight robot to keep a distance from the obstacle, which can serve as a warning. The guidance target item can enable the flight robot to quickly complete the command on the premise of ensuring its own safety.

The following formula is used to establish the obstacle avoidance model of the flight manipulator by using the Gaussian distribution:

$$g_{ob}\left(E_{F\rho}\right) = -\frac{1}{\sqrt{2\pi}} f^{-\frac{E_{F\rho}^2}{2}} \tag{1}$$

Among them, F is the end position of the flight manipulator; ρ is the position of obstacles encountered by the flight manipulator during the execution of the command; $F\rho$ represents the relative distance between the end of the flight manipulator and the obstacle. The smaller the relative distance, the higher the risk faced by the flight manipulator.

The ternary loss function is used to establish the guidance target item model:

$$g_{tr}\left(E_{F\rho}, E_{FS}\right) = \left[E_{F\rho}^2 - E_{FS}^2 - \sigma\right]_+ \tag{2}$$

Among them, S is the target point for the set flight manipulator to execute the command; FS is the relative distance between the end of the flight mechanical arm and the target point of executing the command; σ is the smaller interval between $E_{F\rho}$ and E_{FS}; $\left[E_{F\rho}^2 - E_{FS}^2 - \sigma\right]_+$ means that when the calculation result of $\left[E_{F\rho}^2 - E_{FS}^2 - \sigma\right]$ is greater than 0, the loss function value would output normally. Otherwise, the output is 0.

Combined with obstacle avoidance item and guidance target item, the calculation method of DL position reward function is as follows:

$$\lambda_{location}\left(E_{F\rho}, E_{FS}\right) = g_{ob}\left(E_{F\rho}\right) + g_{tr}\left(E_{F\rho}, E_{FS}\right) \tag{3}$$

2) Direction reward function. The direction reward function model is established by using Coulomb's law. The relationship between the end of the flight manipulator and the obstacles encountered in the execution of instructions is analogized to the mutual exclusion of the same kind of charges. The relationship between the end of the flight manipulator and the task target point is analogized to the mutual attraction of the same kind of charges. The trajectory planning phenomenon of the flight manipulator is regarded as the attraction and exclusion of charges, as shown in Figure 1.

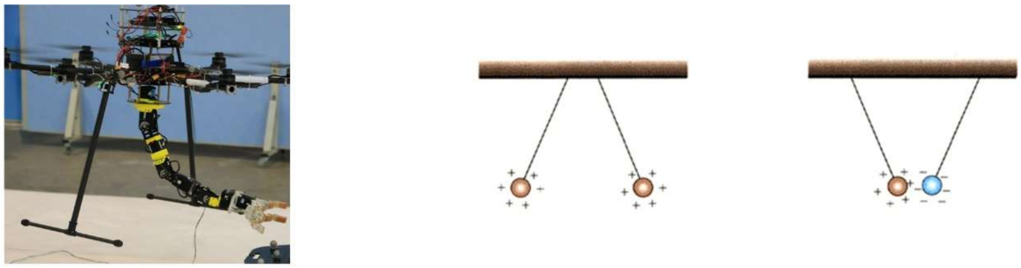

The phenomenon of trajectory planning of flying robotic arms

The phenomenon of attraction and repulsion between charges

Fig. 1. Analogy of the trajectory planning phenomenon of a robotic arm

The attraction and repulsion vectors are as follows:

$$FS' = \frac{J_F J_S}{u_1^2}\frac{FS}{|FS|} \tag{4}$$

$$F\rho' = \frac{J_F J_\rho}{u_2^2}\frac{F\rho}{|F\rho|} \tag{5}$$

Among them, FS' is the attraction vector of the task target point; $F\rho'$ is the repulsion vector of the obstacle; u_1 represents the distance from the end of the flight manipulator to the target point of the mission; u_2 indicates the distance from the end of the flight manipulator to the obstacle.

FC is set as the desired flight manipulator motion vector, and FD is the current flight manipulator motion vector. If the included angle between them is υ, the calculation formula of $\upsilon$is as follows:

$$\upsilon = \arccos\frac{(F\rho' + FS')\bullet FD}{|F\rho' + FS'||FD|} \tag{6}$$

The direction reward function is calculated as follows:

$$\lambda_{orientatin(\upsilon)} = \mu - \frac{\upsilon * \pi}{180} \tag{7}$$

Among them, μ is the forward compensation parameter.

3) Deep learning location reward function. By considering the influence of obstacles and target points on the trajectory planning of the flight manipulator, the expression formulas of the bearing reward function are as follows:

$$\lambda_{global} = \begin{bmatrix} \lambda_{location}(E_{F\rho}, E_{FS}) \\ \lambda_{orientation}(\upsilon) \end{bmatrix} \tag{8}$$

$$\lambda = \xi\lambda_{global} = \begin{bmatrix} \xi_{location} \\ \xi_{orientation} \end{bmatrix}^S \begin{bmatrix} \lambda_{location}(E_{F\rho}, E_{FS}) \\ \lambda_{orientation}(\upsilon) \end{bmatrix} \tag{9}$$

Among them, λ_{global} is the combination of direction reward and position reward, and ξ is the weight vector.

3. Servo Control of Flight Manipulator Based on Image Moment and Vector Product Method

1) Image jacobian matrix of image moments. Image moments can represent the global characteristics of an image. In general, the calculation formula of image moments is as follows:

$$n_{pq} = \int\int_{\varpi} P(v,w) v^p w^q evew \tag{10}$$

Among them, $P(v,w)$ represents the gray value of the image pixel, and ϖ represents the image plane area.

When the gray value of the image pixel is set to be unchanged in motion, the servo control of the flight manipulator is as follows:

$$\dot{n}_{pq} = H_{n_{pq}} \dot{V}_k \tag{11}$$

Among them, $\dot{n}_{pq}$ represents the selected image moment feature vector, and $H_{n_{pq}}$ represents the image Jacobian matrix. The calculation formula is as follows:

$$H_{n_{pq}} = [n_{rv} \ n_{rw} \ n_{rz}] \tag{12}$$

The p and q are valued, and some moments obtained are taken as image features. When the values of p and q are set to 0, the image matrix H_{α} related to the object area α is obtained, and the feature vector of the area α is as follows:

$$\alpha = n_{00} \tag{13}$$

If the values of p and q are set to 1, n_{10} and n_{01} are obtained. The barycentric coordinates of the image are as follows:

$$v_g = n_{10} / n_{00} \tag{14}$$

$$w_g = n_{01} / n_{00} \tag{15}$$

The barycentric coordinates and area coordinates of the image matrix can represent the actual position of an object in reality. The image feature vector is set to $t = [v_g, w_g, \alpha]^S$, and the desired image is set to $t^* = [v_g^*, w_g^*, \alpha^*]^S$. The image Jacobian matrix can be expressed as follows:

$$H_{n_{pq}} = H(t,Z) = \begin{bmatrix} -\frac{1}{Z} & 0 & \frac{v_g}{Z} \\ 0 & -\frac{1}{Z} & \frac{w_g}{Z} \\ 0 & 0 & \alpha\left(\frac{3}{Z-K}\right) \end{bmatrix} \tag{16}$$

The image jacobian matrix $H(t^*, Z^*)$ at the desired position is taken as an estimate of the image jacobian matrix.

2) Jacobian matrix of flight manipulator based on vector product. From the perspective of manipulator dynamics, since the camera is fixed at the end of the mechanical arm, the speed at the

end of the manipulator is the same as that of the camera. From this perspective, the Jacobian matrix of the manipulator can be defined as follows:

$$Q_k = \begin{bmatrix} \dot{V}_k & \xi \end{bmatrix}^S / \dot{\theta} \tag{17}$$

Among them, ξ represents the angular velocity of the end joint of the flight manipulator.

Before using the vector product method to solve Q_k, the initial position of the flight manipulator should be set. According to the specific structure of the flight manipulator and the number of manipulators, the Denavit Hartenberg method is used to determine the coordinate system of the rotation joint of the flight manipulator, and the base coordinate system of the flight manipulator and the coordinate system of the rotation joint of each manipulator should be established. After the joint coordinate system is established, the Denavit Hartenberg parameter table of the manipulator rotation joint is determined according to the adjacent joint coordinate system. Denavit Hartenberg parameter table is actually the transformation relationship table of the coordinates of adjacent joints. According to the coordinate system established for each joint before and according to the transformation rules, the D-H parameter table can be obtained. By taking the end effector of the flight manipulator as the object for analysis, the speed of the end effector of the flight manipulator can be expressed as the velocity vector, translation motion vector, and rotation angular velocity vector of all rotation joint coordinate points in the coordinate system, which are expressed as follows with the formulas:

$$x_m = \left(Z_m * {}^n I_m^0\right)^* j\, m \tag{18}$$

$$y_m = Z_m \overset{*}{j}\, m \tag{19}$$

$$Q_m = \begin{bmatrix} Z_m * {}^m I_m^0 \\ Z_m \end{bmatrix} \tag{20}$$

Among them, m represents the number of coordinate points of the rotation joint of the flight manipulator; Z_m is the unit vector in the m-th coordinate system and in the Z-axis; ${}^m I_m^0 = {}_m^0 U \bullet {}^m I_m^m$.

The transformation matrix of the coordinate system of adjacent joints of the flight manipulator is as follows:

$$\begin{aligned} &{}^m S_{m+1} = B_{m+1} = \\ &\begin{bmatrix} k_{m+1} & -t_{m+1} ka_{m+1} & t_{m+1} ta_{m+1} & a_{m+1} k_{m+1} \\ t_{m+1} & k_{m+1} ka_{m+1} & -k_{m+1} ta_{m+1} & a_{m+1} t_{m+1} \\ 0 & ta_{m+1} & ka_{m+1} & e_{m+1} \\ 0 & 0 & 0 & 0 \end{bmatrix} \end{aligned} \tag{21}$$

Among them, ${}^m S_{m+1}$ represents the transformation from coordinate system m to m+1, and this transformation is marked as B_{m+1}; ta_{m+1} means $\sin a_{m+1}$; ka_{m+1} is denoted as $\cos a_{m+1}$.

${}^0 S_m$ is the transformation matrix of the coordinate system of joint m relative to the base, and ${}_m^0 U$ is the upper left corner ${}^0 S_m$ of 3×3. The Jacobian matrix 88 of the mechanical arm can be obtained from ${}^0 S_m$, Z_m, ${}_m^0 U$, ${}^m S_{m+1}$, etc

$$\begin{cases} Q_k = [Q_1 \ Q_2 \ \cdots_1 \ Q_m \ ] \\ Q_m = \begin{bmatrix} Z_m *^m I_m^0 \\ Z_m \end{bmatrix} \end{cases} \tag{22}$$

4. Data Encryption of Flying Robots Based on Blockchain

The data of some flying robots is related to the sensitive data monitored on site. For enterprises, data leakage would affect their business safety; for individuals, the disclosure of data is related to their privacy and security. However, due to the lack of information interaction steps, errors in the information replacement process and poor encryption effect in the traditional flight robot data encryption transmission, the sensor data collected by the flight robot in the task process is easy to be tampered and destroyed by human beings. The blockchain has the core features of data tamper prevention and data decentralization. The blockchain has a good application prospect in the field of flight robot data encryption transmission. This paper has studied the flight robot data encryption based on the blockchain.

1) Overall architecture of flight robot data encryption system based on blockchain. The overall architecture of the flight robot data encryption system includes five parts, as shown in Figure 2. They are driving mechanism, flight robot data encryption control system, service function module, blockchain interaction module and trusted data storage module.

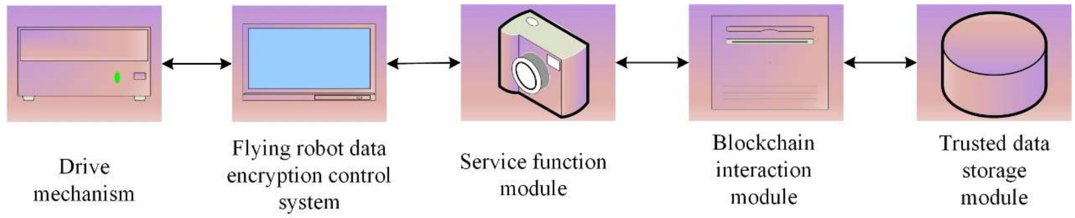

Fig. 2. The overall architecture of the flying robot data encryption system

Driving mechanism: It would execute corresponding actions after receiving the command from the flight robot control system, which plays a role in real-time monitoring, real-time detection, etc. It can feed back the monitored data information to the flight robot control system in time. Flight robot data encryption control system: It can ensure that the motion of the flight robot and the mechanical arm meets the predetermined requirements by timely adjusting the driving mechanism by processing the monitoring information fed back by the driving mechanism and comparing it with the preset information. Service function module: The remote video service can expand the scope of video monitoring, which enables the flight robot control system to sense the changes of external environmental conditions in a timely manner. It can improve the moving accuracy of the flying robot, including the moving accuracy of the aircraft and the operating accuracy of the manipulator. Blockchain interaction module: It can realize the distributed management of data and make use of the decentralized characteristics of blockchain technology, so that the data storage of interactive information can be directly processed through the verification node cluster and the management of third-party institutions is removed. The blockchain interaction module can ensure the database security. There are complete data records in each verification node. Even if some node data is lost, the flight robot control system can still work. When attacked by external data, blockchain technology uses encryption technology to sign data, so that information would not be tampered with. Trusted data storage module: Its function is to store instructions and data, and its data can be directly and randomly accessed by the central processor.

2) Information signature verification mechanism. In the blockchain technology, there is no center to command and coordinate each accounting node. Each node has an independent ledger, and achieves joint bookkeeping by keeping the ledger synchronized. In the case of complex and changeable network states, information signature verification mechanism should be introduced for malicious operations that nodes may face to ensure that the spatially distributed account books of each node can be identical. The information signature verification mechanism is shown in Figure 3.

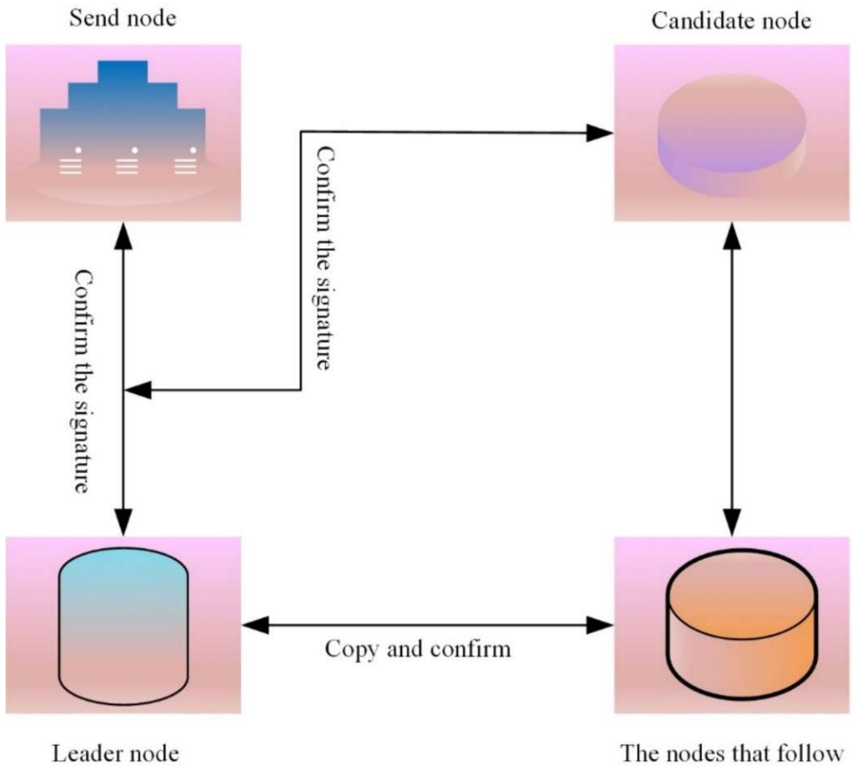

Fig. 3. Information signature verification mechanism

As shown in Figure 3, the information signature verification mechanism mainly includes three main contents: After confirming that the sending node is normal, the information signature verification mechanism sends the information to the leading node; after being copied and confirmed, the leader node sends the information to the follower node; after signature confirmation of sending node and leading node, the information signature verification mechanism can send the result to the candidate node.

5. Experimental Investigation on Trajectory Planning and Control of Flight Manipulator

Two flight manipulators are selected. One flight manipulator uses the traditional trajectory planning method, and the other flight manipulator uses the DL based trajectory planning method to issue five commands to the flight manipulator. It evaluates the traditional trajectory planning method and the DL trajectory planning method from the collision evaluation index of the flight manipulator, the speed evaluation index of the flight manipulator reaching the target point, and the comprehensive evaluation index combining the number of collisions and the time of reaching the target point.

The collision test of the flight manipulator is conducted and evaluated according to the test results. The results of the five evaluations are shown in Figure 4.

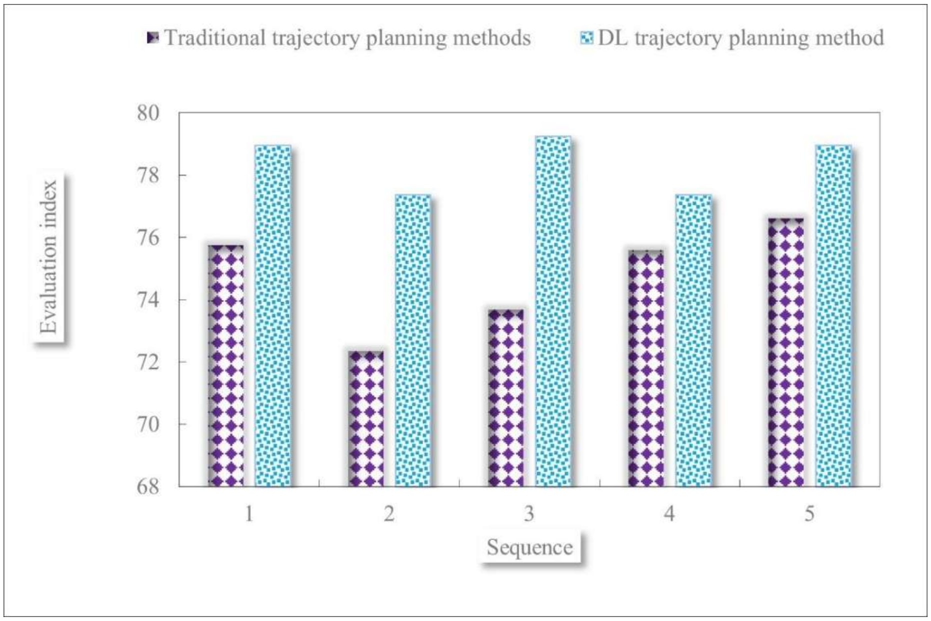

Fig. 4. Flying robotic arm crash test

As shown in Figure 4, in the first test, the impact test evaluation index of the flight manipulator under the traditional trajectory planning method is 75.76, and the impact test evaluation index of the flight manipulator under the DL trajectory planning method is 78.96. The impact test evaluation index of the flight manipulator under the DL trajectory planning method is 3.2 higher than that under the traditional trajectory planning method. It can be clearly seen that the impact test results of the flight manipulator under the DL trajectory planning method are better. In the second test, the impact test evaluation index of the flight manipulator under the traditional trajectory planning method is 72.35, and the impact test evaluation index of the flight manipulator under the DL trajectory planning method is 77.36. The collision test evaluation index of flight robot arm under DL trajectory planning method is 5.01 higher than that under traditional trajectory planning method, and there is a certain gap between the collision test results of the two methods. The average flight robot collision test evaluation index of the five tests under the traditional trajectory planning method is 74.8, and the average flight robot collision test evaluation index of the five tests under the DL trajectory planning method is 78.38. The average flight robot collision test evaluation index under the DL trajectory planning method is 3.58 higher than the average flight robot collision test evaluation index under the traditional trajectory planning method, with the proportion of 4.79% higher. It shows that the DL trajectory planning method can play a certain role in avoiding the collision of the flying robot arm.

The speed test of the flight manipulator reaching the target point is conducted, and the evaluation is conducted according to the test effect. The evaluation results are shown in Figure 5.

Fig. 5. Speed test at which the flying robotic arm reaches the target point

As shown in Figure 5, in the fifth test, the speed evaluation index of the flight manipulator under the traditional trajectory planning method is 73.67, and the speed evaluation index of the flight manipulator under the DL trajectory planning method is 77.13. The speed evaluation index of the flight manipulator under the DL trajectory planning method is 3.46 higher than that under the traditional trajectory planning method. From the fifth result, it can be seen that the DL trajectory planning method has more advantages than the traditional trajectory planning method. After five tests, the average speed evaluation index of the flight manipulator under the traditional trajectory planning method is 73.22, and the average speed evaluation index of the flight manipulator under the DL trajectory planning method is 76.63. The speed evaluation index of the average flight manipulator under the DL trajectory planning method is 3.41 higher than that under the traditional trajectory planning method, with the proportion of 4.66% higher. It shows that compared with the traditional trajectory planning method, the DL trajectory planning method can play a more important role in improving the speed of the flight manipulator.

The comprehensive evaluation is carried out based on the results of collision test and speed test of the flight robot arm. The evaluation results are shown in Figure 6.

Fig. 6. Comprehensive test evaluation of flying manipulator

As shown in Figure 6, on the whole, the comprehensive test evaluation index of the flight manipulator under the DL trajectory planning method is higher than that under the traditional trajectory planning method. From the specific data, in the first test, the comprehensive test evaluation index of the flight manipulator under the traditional trajectory planning method is 74.03, and the comprehensive test evaluation index of the flight manipulator under the DL trajectory planning method is 77.69. There is a clear gap between the two. In the fifth test, the comprehensive test evaluation index of the flight manipulator under the traditional trajectory planning method is 75.15, and the comprehensive test evaluation index of the flight manipulator under the DL trajectory planning method is 78.04. The difference between the two values is 2.89. From the average results of the five tests, the average comprehensive test evaluation index of the flight manipulator under the traditional trajectory planning method is 74.02, and the average comprehensive test evaluation index of the flight manipulator under the DL trajectory planning method is 77.51. The comprehensive test evaluation index of the average flight manipulator under the DL trajectory planning method is 3.49 higher than that under the traditional trajectory planning method, with a higher proportion of 4.71%. This shows that compared with the traditional trajectory planning method, the DL trajectory planning method can improve the trajectory planning effect of the flight manipulator.

The data security of the flying robot is tested, and the data security capability of the blockchain technology is observed by tampering, destroying and other attacks on the data of the flying robot. The flight robot data system using blockchain technology and the flight robot data system using conventional technology are attacked five times respectively, and the evaluation results are shown in Table 1.

Table 1. Data security testing of flying robots

	Conventional technology	Blockchain technology
1	72.54	78.61
2	72.39	78.43
3	78.41	79.37
4	72.49	80.12
5	74.37	79.34

As shown in Table 1, during the first attack test, the flight robot data security evaluation index using conventional technology is 72.54, and the flight robot data security evaluation index using blockchain technology is 78.61. The data security evaluation index of flying robots using blockchain technology is higher than that of flying robots using conventional technology. From the average results of the five attack tests, the flight robot data security evaluation index using conventional technology is 74.04, and the flight robot data security evaluation index using blockchain technology is 79.17. The data security evaluation index of flying robots using blockchain technology is 5.13 higher than that of flying robots using conventional technology, with the proportion of 6.93% higher. This shows that compared with conventional technology, blockchain technology has more advantages in ensuring the data security of flying robots.

6. Conclusions

In this paper, the obstacle avoidance model of the flight manipulator was established by using Gaussian distribution, the direction reward function model was established by using Coulomb's law, and the image Jacobian matrix based on image moment and the flight manipulator Jacobian matrix based on vector product were constructed. This paper briefly discussed the application of blockchain technology in the field of flight robot data, and carried out experimental research on TPC of flight robot. The conclusions were as follows: Compared with the traditional trajectory planning method, DL trajectory planning method was more conducive to improving the obstacle avoidance ability of the flight manipulator, and DL trajectory planning method had certain advantages in improving the task completion speed of the flight manipulator. Compared with conventional technologies, blockchain technology was more conducive to ensuring the data security of flying robots.

Funding

This work was supported by the National Natural Science Foundation of Shandong (Grant No. ZR2019MEEO59).

References

[1] Hassanalian, M., & Abdelkefi, A. (2017). Classifications, applications, and design challenges of drones: A review. Progress in Aerospace sciences, 91, 99-131.

[2] Fan, J., & Saadeghvaziri, M. A. (2019). Applications of drones in infrastructures: Challenges and opportunities. International Journal of Mechanical and Mechatronics Engineering, 13(10), 649-655.

[3] Dileep, M. R., Navaneeth, A. V., Ullagaddi, S., & Danti, A. (2020, November). A study and analysis on various types of agricultural drones and its applications. In 2020 fifth international conference on research in computational intelligence and communication networks (ICRCICN) (pp. 181-185). IEEE.

[4] Mohd Noor, N., Abdullah, A., & Hashim, M. (2018, July). Remote sensing UAV/drones and its applications for urban areas: A review. In IOP conference series: Earth and environmental science (Vol. 169, p. 012003). IOP Publishing.

[5] Chan, K. W., Nirmal, U., & Cheaw, W. G. (2018, November). Progress on drone technology and their applications: A comprehensive review. In AIP conference proceedings (Vol. 2030, No. 1). AIP Publishing.

[6] Otto, A., Agatz, N., Campbell, J., Golden, B., & Pesch, E. (2018). Optimization approaches for civil applications of unmanned aerial vehicles (UAVs) or aerial drones: A survey. Networks, 72(4), 411-458.

[7] Li, Y., & Liu, C. (2019). Applications of multirotor drone technologies in construction management. International Journal of Construction Management, 19(5), 401-412.

[8] Vidyadhara, B. V., Tony, L. A., Gadde, M. S., Jana, S., Varun, V. P., Bhise, A. A., ... & Ghose, D. (2022). Design and integration of a drone based passive manipulator for capturing flying targets. Robotica, 40(7), 2349-2364.

[9] Kachroo, A., Thornton, C. A., Sarker, M. A. R., Choi, W., Bai, H., Song, I., ... & Ekin, S. (2021). Emulating UAV motion by utilizing robotic arm for mmWave wireless channel characterization. IEEE Transactions on Antennas and Propagation, 69(10), 6691-6701.

[10] Kim, S. J., Lee, D. Y., Jung, G. P., & Cho, K. J. (2018). An origami-inspired, self-locking robotic arm that can be folded flat. Science Robotics, 3(16), eaar2915.

[11] Ibrahim, I. N., Al Akkad, M. A., & Abramov, I. V. (2017, June). Attitude and altitude stabilization of a microcopter equipped with a robotic arm. In 2017 International Siberian Conference on Control and Communications (SIBCON) (pp. 1-8). IEEE.

[12] Suthar, B., & Jung, S. (2021). Design and feasibility analysis of a foldable robot arm for drones using a twisted string actuator: Frad-tsa. IEEE Robotics and Automation Letters, 6(3), 5769-5775.

[13] Pan, S., & Endo, G. (2021). Toward mission-dependent long robotic arm enhancement: design method of flying watch attachment allocation based on thrust drivability. ROBOMECH Journal, 8, 1-22.

[14] Paul, H., Ono, K., Ladig, R., & Shimonomura, K. (2018, July). A multirotor platform employing a three-axis vertical articulated robotic arm for aerial manipulation tasks. In 2018 IEEE/ASME International Conference on Advanced Intelligent Mechatronics (AIM) (pp. 478-485). IEEE.

[15] Ryll, M., Muscio, G., Pierri, F., Cataldi, E., Antonelli, G., Caccavale, F., ... & Franchi, A. (2019). 6D interaction control with aerial robots: The flying end-effector paradigm. The International Journal of Robotics Research, 38(9), 1045-1062.

[16] Kim, S., Seo, H., Shin, J., & Kim, H. J. (2018). Cooperative aerial manipulation using multirotors with multi-dof robotic arms. IEEE/ASME Transactions on Mechatronics, 23(2), 702-713.

[17] Chen, A., Song, B., Wang, Z., Xue, D., & Liu, K. (2022). A novel actuation strategy for an agile bioinspired FWAV performing a morphing-coupled wingbeat pattern. IEEE Transactions on Robotics, 39(1), 452-469.

[18] Palmieri, P., Melchiorre, M., & Mauro, S. (2022). Design of a lightweight and deployable soft robotic arm. Robotics, 11(5), 88.

[19] Hingston, L., Mace, J., Buzzatto, J., & Liarokapis, M. (2020, November). Reconfigurable, adaptive, lightweight grasping mechanisms for aerial robotic platforms. In 2020 IEEE International Symposium on Safety, Security, and Rescue Robotics (SSRR) (pp. 169-175). IEEE.

[20] Suarez, A., Heredia, G., & Ollero, A. (2018). Design of an anthropomorphic, compliant, and lightweight dual arm for aerial manipulation. IEEE Access, 6, 29173-29189.

[21] Suarez, A., Jimenez-Cano, A. E., Vega, V. M., Heredia, G., Rodriguez-Castaño, A., & Ollero, A. (2018). Design of a lightweight dual arm system for aerial manipulation. Mechatronics, 50, 30-44.

[22] Marolla, M., Cacace, J., & Lippiello, V. (2023). Design and Control of a Novel High Payload Light Arm for Heavy Aerial Manipulation Tasks. In ICINCO (1) (pp. 465-473).

[23] Sun, H., Zhang, W., Yu, R., & Zhang, Y. (2021). Motion planning for mobile robots—Focusing on deep reinforcement learning: A systematic review. IEEE Access, 9, 69061-69081.

[24] Ma, J., Chen, P., Xiong, X., Zhang, L., Yu, S., & Zhang, D. (2024). Research on Vision-Based Servoing and Trajectory Prediction Strategy for Capturing Illegal Drones. Drones, 8(4), 127.

[25] Dai, Y., Xiang, C., Zhang, Y., Jiang, Y., Qu, W., & Zhang, Q. (2022). A review of spatial robotic arm trajectory planning. Aerospace, 9(7), 361.